

pubs.acs.org/estengg Article

Evaluating the Performance of Using Low-Cost Sensors to Calibrate for Cross-Sensitivities in a Multipollutant Network

Misti Levy Zamora,* Colby Buehler, Hao Lei, Abhirup Datta, Fulizi Xiong, Drew R. Gentner, and Kirsten Koehler



Cite This: ACS EST Engg. 2022, 2, 780-793



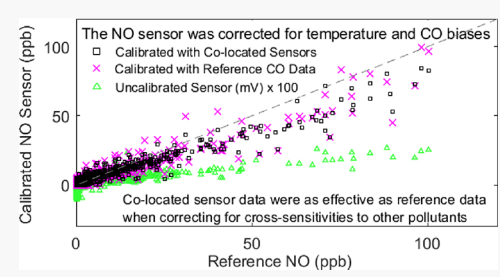
ACCESS I

III Metrics & More

Article Recommendations

s Supporting Information

ABSTRACT: As part of our low-cost sensor network, we colocated multipollutant monitors containing sensors for particulate matter, carbon monoxide, ozone, nitrogen dioxide, and nitrogen monoxide at a reference field site in Baltimore, MD, for 1 year. The first 6 months were used for training multiple regression models, and the second 6 months were used to evaluate the models. The models produced accurate hourly concentrations for all sensors except ozone, which likely requires nonlinear methods to capture peak summer concentrations. The models for all five pollutants produced high Pearson correlation coefficients (r > 0.85), and the hourly averaged calibrated sensor and reference concentrations from the evaluation period were within 3–12%. Each sensor required a distinct set of predictors to



achieve the lowest possible root-mean-square error (RMSE). All five sensors responded to environmental factors, and three sensors exhibited cross-sensitives to another air pollutant. We compared the RMSE from models (NO₂, O₃, and NO) that used colocated regulatory instruments and colocated sensors as predictors to address the cross-sensitivities to another gas, and the corresponding model RMSEs for the three gas models were all within 0.5 ppb. This indicates that low-cost sensor networks can yield useable data if the monitoring package is designed to comeasure key predictors. This is key for the utilization of low-cost sensors by diverse audiences since this does not require continual access to regulatory grade instruments.

KEYWORDS: low-cost sensor, calibration, Plantower, AlphaSense, regression models

1. INTRODUCTION

The expansion of low-cost sensors in recent years has enabled opportunities for ambient air quality monitoring using highly granular networks in urban environments. 1-5 These low-cost sensors have several advantages over traditional instrumentation, such as a substantially lower unit price, compact size, portability, and the ability to capture high spatiotemporal variability. 2,3,6-9 Traditionally, air quality measurements have been collected with the federal reference method (FRM) or federal equivalent method (FEM) instruments that have undergone rigorous testing, and while the precision, accuracy, and lifetime of low-cost sensors are less than those of FRM or FEM, there are numerous benefits to deploying more, less accurate sensor nodes compared to only a few highly accurate instruments. 1-5,8 However, questions persist about the quality of low-cost sensor data. These sensors often report a voltage or resistance instead of a concentration, and it is up to the user to convert the values to useable concentrations. Low-cost sensors often have the added difficulty of needing unit-specific correction factors (CFs), and the sensors are often responsive to numerous factors [e.g., other pollutants, temperature, relative humidity (RH), and pressure]. 9-12 Unit-specific CFs are often needed because the raw output values differ between units, but the responses to an environmental factor are often consistent between units. For many sensors, limited information is provided by the manufacturer about how to best convert the raw sensor data or to correct for interfering environmental factors or cross-sensitivities to other pollutants. Also, if the low-cost sensor produces concentrations, typically, little information is provided about what steps were taken to produce those values. An ongoing issue being discussed in the sensor community is the acceptable level of data manipulation or "postprocessing" that can be employed when correcting lowcost sensor data. 8,13 Hagler et al. 8 emphasized that if data from low-cost sensors are substantially manipulated, it changes from being a true direct measurement to a predictive statistical model. These results are still useful, but there needs to be transparency about the postprocessing methodology. Concerns also exist about "overfitting" the data, where the calibration procedures and models are only appropriate for a specific scenario or location and not applicable to other data sets. 14 In addition, advanced machine learning approaches have been used to calibrate low-cost sensors, but the results are often

Received: October 5, 2021 Revised: March 22, 2022 Accepted: March 23, 2022 Published: April 11, 2022





harder to interpret because the way that the data is handled is not easily explained. 15,16

Examples of calibration methods include exposing the sensors to known concentrations in a controlled laboratory setting or colocating the sensors with reference instruments at a location with similar conditions as the intended measurement location. 2,3,8,16-19 Laboratory calibration allows for sensors to be exposed to one pollutant or a mixture of pollutants in a regulated environment, which can yield valuable insights into the response of the sensor to those factors. However, a sensor may be responsive to many pollutants, which may change as a function of temperature and/or RH. It is often cost- and timeprohibitive to collect data on every known pollutant's crosssensitivity under a range of realistic environmental conditions. Therefore, many low-cost sensors are colocated with highprecision reference instruments at a field site to assess the performance under ambient conditions. ^{3,12,18,20–25} Governmental reference field sites often have the added benefit of operating instruments for several regulated pollutants, permitting the comparison of the low-cost sensor data with several pollutants to identify cross-sensitives. A low-cost sensor must be evaluated for cross-sensitives since a sensor may respond to other factors at an equal or greater magnitude, potentially resulting in large errors if not accounted for in postprocessing.¹⁸ To date, less is known about how effective calibrations are when cross-sensitives are corrected using only other low-cost sensors as predictors in direct comparison to using reference data.

The Solutions to Energy, AiR, Climate, and Health (SEARCH) Center has installed 45 low-cost multipollutant monitors in Baltimore, Maryland, USA, where little is known about the variability of air pollutants throughout the city. 9,26-30 The central goal of this specific work was to identify the key factors that influence the sensor responses for five low-cost sensors [particulate matter smaller than 2.5 μ m (PM_{2.5}), carbon monoxide (CO), ozone (O₃), nitrogen dioxide (NO₂), and nitrogen monoxide (NO)] that are installed in our multipollutant monitors. Specifically, we aim to identify the environmental factors that influence the responses of each sensor, identify cross-sensitivities to other common pollutants, develop and apply multiple calibration models, and evaluate the accuracies of calibration models with colocated sensor data as predictors compared to calibration models utilizing reference data as predictors.

2. METHODS

2.1. Measurement Location. Data from two SEARCH multipollutant monitors were used in this work. They were concurrently installed at two Maryland Department of the Environment (MDE) sites; one at Oldtown (ID = 245100040; 39.298056, -76.604722) in Baltimore City, Maryland, and one at Essex (ID = 240053001; 39.310833, -76.474444) in Baltimore County, Maryland (approximately 11 km east of the Oldtown site). The Oldtown site was about 5 m above ground level and 10 m from a major intersection.³¹ The annual average daily traffic count in 2017 was 11,351. The Essex site was about 5 m above ground level and 5 m from a residential street. The Essex site is categorized as suburban, with a lower traffic count of 2190. Reference data from the PM_{2.5} instrument (Met One BAM-1020) at the Oldtown site and CO (Teledyne API 300EU), O₃ (Teledyne API model 400), NO₂ (Teledyne API 200EU), and NO (Teledyne API 200EU) at the Essex site were used for comparison with the colocated sensor in these

analyses. Both reference sites also measure meteorological parameters (hourly averaged temperature, vector-averaged wind speed, vector-averaged wind direction, atmospheric pressure, RH, and precipitation). This manuscript focuses on data collected from February 1, 2019, to February 1, 2020.

2.2. Sensors. Here the term monitor is used to describe a multipollutant instrument that comprises multiple sensors, while the term sensor is used to describe the individual sensing components. The SEARCH monitor has been described in detail by Buehler et al.⁹ and in the Supporting Information. Briefly, a suite of sensors is built into a multipollutant stationary monitor that measures the concentrations of CO (AlphaSense CO-A4 sensor), NO₂ (AlphaSense NO2-A43F), NO (NO-A4), CO₂ (AlphaSense IRC-A1), O₃ (MiCS-2614), methane (CH₄, Figaro TGS 2600), particulate matter (PM; Plantower PMS A003), RH (Sensirion SHT25), and temperature (T; Sensirion SHT25). Since CO₂ and CH₄ are not measured at the MDE sites, they were not considered here. In this work, the uncorrected CO, NO2, and NO sensor (in voltage) were the difference between the working electrode and the auxiliary electrode, the ozone sensor was the resistance directly reported by the sensor (ohms, Ω), and the uncalibrated PM_{2.5} sensor used the built-in atmospheric environment CF "atmos" since the manufacturer indicated it was for outdoor environments. The electronics for the multipollutant monitor were designed to have modularized functions on each circuit board, and each sensor has a designated analog circuitry to supply power, amplify signals, and filter noise. The SHT25 temperature/RH sensor was located at the front of the gas manifold to measure the conditions observed by the gas sensors, which will be offset but dependent on the ambient conditions. For that reason, we used this RH and temperature to calibrate these sensors. Measurements were collected every 160 ms for each sensor, transmitted as 10 s averages, and then the data were converted into 1 h averages to correspond with the resolution of the available reference data. In this manuscript, the term average refers to the arithmetic mean. The monitor has separate inlets for particles and gases. Owing to an inlet issue affecting the gas sensors on the Essex monitor during the winter of 2019, the O₃, NO₂, and NO sensor data were unavailable between December 20, 2019, and February 1, 2020. Therefore, the analyses for these sensors end on December 19, 2019.

2.3. Multiple Linear Regressions. 2.3.1. Calibration Model Development. To cover a range of concentrations and environmental conditions in warm and cold seasons and pollutant concentrations, the first 6 months (February 1 to July 31, 2019) were set aside as the "training period" for the multiple regression models [multiple linear regression (MLR)], and August 1, 2019, to February 1, 2020, was used as the "evaluation period". Hourly averages were used for all data sets. A generic MLR model used to calibrate the low-cost sensors is given by

$$\begin{aligned} & \operatorname{reference_{Pollutant}}(t) \\ &= \beta_0 + \beta_1 * \operatorname{sensor_{Pollutant}}(t) + \sum_{1}^{n} \beta_n * \operatorname{predictor_n}(t) \end{aligned} \tag{1}$$

where reference_{Pollutant} is the reference concentration at time t for a given pollutant, β_0 is the constant intercept, β_1 is the coefficient applied to the uncalibrated sensor value for a given pollutant at time t, and β_n is the coefficient applied to predictor_n. Predictors that were considered in the models

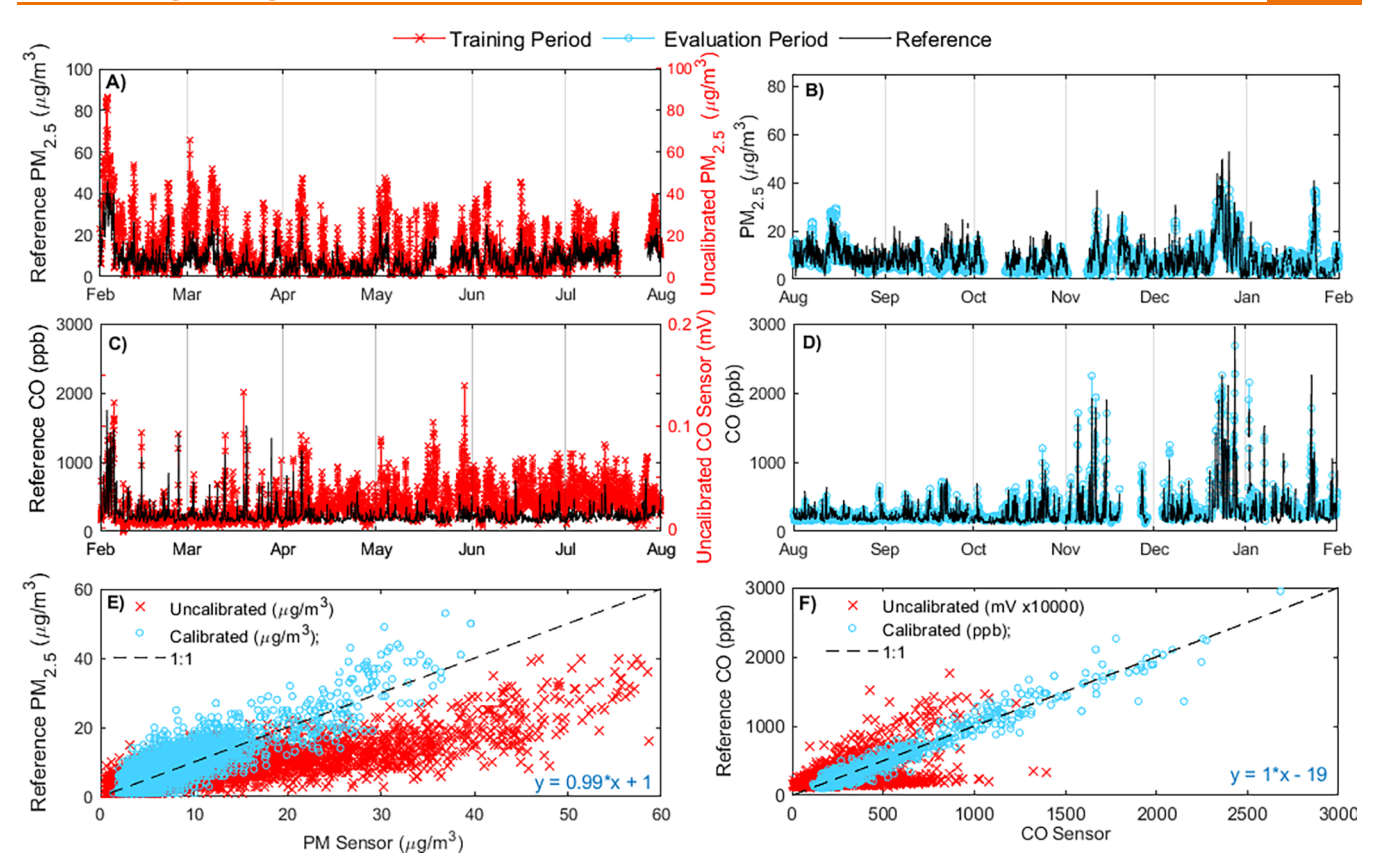


Figure 1. (A–D) Time series of the hourly averaged reference (black) and PM_{2.5} and CO sensor data from the training (uncalibrated data displayed in red; left column) and evaluation (calibrated displayed in blue; right column) periods. The uncorrected CO sensor (in mV) is the difference between the working electrode and the auxiliary electrode. (E,F) Scatterplots of the sensor vs reference data from the two periods. Note: the raw sensor values shown here are specific to this individual sensor and not representative of all sensors of the same type, but the responses (e.g., reducing output because of exposure to a pollutant or changing environmental conditions) should be similar across different sensor of the same type. The linear fits for the evaluation periods are displayed.

included: temperature, RH, PM_{2.5}, CO, O₃, NO₂, NO, an interaction term between the sensor and temperature, an interaction term between the sensor and RH, time, an interaction term between the sensor and time, daylight hours (a binary variable which is 1 between 6 AM and 7 PM and 0 otherwise), and weekday (a binary variable i.e., 1 on Saturdays and Sundays and 0 otherwise). If a sensor exhibited a crosssensitivity to another pollutant, two models were developed for that sensor: (1) a calibration model with colocated reference data as the cross-sensitive pollutant predictor and (2) a calibration model with the uncalibrated colocated sensor data as the cross-sensitive pollutant predictor. Only significant predictors, defined here as p < 0.05, were retained in the final model. If a predictor (e.g., RH) exhibited nonlinearity, the predictor squared (RH²) was evaluated as a potential predictor. If a predictor exhibited piecewise linear responses (also known as a "broken arrow" response), a spline was introduced at the median value. In the case where a global linear or quadratic fit did not capture the relationship adequately, we used splines to model nonlinearity/piecewise linearity. The knot was chosen to be the median value of the predictor or some other value that was at a clear change-point for the relationship. A correlation matrix of the measured pollutant and environmental conditions is shown in Table S1.

The final models were chosen based on the Akaike information criterion (AIC) and Bayesian information criterion (BIC).³² When comparing models, the calibration

model with the lowest BIC was selected. The AIC and BIC penalize based on the number of parameters in the model; thus, more parsimonious models have lower values and are preferred. BIC introduces stronger penalties than the AIC, which may help limit overfitting. If the BIC was similar between the two models, the root-mean-square error (RMSE; Equation 2) from the training period was used to identify the better model.

$$RMSE = \sqrt{\frac{\sum_{i=1}^{N} (reference_i - predicted_i)^2}{N}}$$
(2)

The RMSE was calculated using eq 2, where reference_i and predicted_i are the corresponding *i*-th 1 h-averaged concentrations from a training or evaluation period with N hourly measurements. An RMSE value of 0 would indicate a perfect agreement between the reference and sensor. We calculated the percent bias with the following

percent bias =
$$100 \times \frac{\sum (predicted_i - reference_i)}{\sum reference_i}$$
 (3)

After the final calibration model was selected for the training period, the coefficients were applied to the data from the evaluation period, and the RMSE and *r* were calculated for the out-of-sample period. All data analyses were conducted using MATLAB 2019a and StataIC 16, and the nonlinear least-

Table 1. Summarized Hourly Pollutant Concentrations and Calibration Model Performance during the Training and Evaluation Periods^a

	Training Period Statistics				Evaluation Period Statistics							
-	Average ±				Average ±							
	Standard	Median			Standard	Median	RMSE					
	Deviation	(5th-95th)	RMSE	r	Deviation	(5th-95th)	(% bias)	r				
$\mathbf{PM_{2.5}} \; (\mu \mathrm{g/m^3})$												
Reference	8.0 ± 6.0	7.0 (1.0–18.0)			8.8 ± 6.0	7.0 (1.0–19.0)						
Uncalibrated Sensor	12.7 ± 12.3	8.8 (1.0-37.5)	9.2	0.84	12.4 ± 11.7	9.2 (1.0-37.4)	8.6 (43%)	0.80				
Calibrated Sensor	8.0 ± 5.4	6.6 (2.4–17.9)	2.8	0.89	8.0 ± 5.0	6.9 (2.5–18.3)	3.4 (-10%)	0.85				
CO (ppb)												
Reference	234 ± 144	197 (137–446)			282 ± 248	203 (134-688)						
Uncalibrated Sensor				0.51				0.84				
Calibrated Sensor	234 ± 128	199 (151–417)	60.5	0.90	297 ± 238	218 (164–688)	58.9 (5.6%)	0.97				
NO_2 (ppb)												
Reference	7.9 ± 7.9	5.0 (1.0-26.0)			8.1 ± 7.0	5.0 (1.0-23.0)						
Uncalibrated Sensor				0.71				0.68				
Calibrated Sensor using Reference Data for Pollutant Predictors	8.1 ± 7.3	5.9 (2.1–23.7)	3.3	0.91	7.8 ± 5.7	5.9 (1.8–19.1)	3.5 (-9.0%)	0.88				
Calibrated Sensor using Sensor Data for Pollutant Predictors	7.9 ± 7.1	5.9 (0.5-23.5)	3.6	0.90	9.4 ± 5.8	7.6 (0.5–20.4)	3.6 (12%)	0.88				
		O ₃ (p	pb)									
Reference	35.5 ± 15.7	36.0 (7.0-60.0)	- /		28.5 ± 14.9	28.0 (4.0-56.0)						
Uncalibrated Sensor		, ,		0.52		, ,		0.52				
Calibrated Sensor using Reference Data for Pollutant Predictors	35.8 ± 13.7	36.5 (10.5–58.1)	6.9	0.90	28.4 ± 13.6	29.8 (7.0-55.8)	7.4 (-7.1%)	0.86				
Calibrated Sensor using Sensor Data for Pollutant Predictors	35.6 ± 13.6	36.1 (9.4–57.6)	7.1	0.90	28.3 ± 15.5	26.6 (3.6–55.5)	7.0 (-4.0%)	0.89				
		NO (p	opb)				, ,					
Reference	3.0 ± 11.0	0.5 (0.1-11.2)			3.3 ± 10.0	0.6 (0.1-16.5)						
Uncalibrated Sensor				0.81				0.77				
Calibrated Sensor using Reference Data for Pollutant Predictors	3.0 ± 10.3	0.6 (0.01–12.3)	3.0	0.96	2.8 ± 8.3	0.5 (0.01–13.7)	3.3 (-15%)	0.96				
Calibrated Sensor using Sensor Data for Pollutant Predictors	3.0 ± 10.0	0.6 (0.01–12.9)	3.4	0.95	3.3 ± 7.8	0.8 (0.01–13.9)	3.2 (-2.7%)	0.97				
Temperature (°C)												
Ambient Reference	15.1 ± 9.7	16.6 (-0.5 to 29.4)			13.0 ± 10.2	11.6 (-1.6 to 28.8)						
Internal Sensor	20.8 ± 10.9	21.8 (3.4-38.4)			19.2 ± 10.6	18.0 (3.1-37.4)						
RH (%)												
Ambient Reference	61.8 ± 19.9	61 (29–91)			65.4 ± 17.6	66 (38–91)						
Internal Sensor	49.8 ± 16.0	49.4 (24.2–73.6)			52.4 ± 13.8	53.4 (30.4–73.0)						

^aIn the case of NO₂, O₃, and NO, only periods when the predictors for both models were available were included in the summary values, which allows for direct comparison.

squares fits were calculated using the curve fitting toolbox with MATLAB 2019a.

2.3.2. Sensor Baseline Signal Drift. To assess sensor drift, specifically, the change in baseline response over time, the significance of the time predictor was evaluated when the concentration was in the lowest quartile of concentrations for each sensor. If the time predictor was significant, there existed some baseline changes that were not accounted for by differences in the other factors (e.g., temperature or other pollutants). The conditions were comparable during both winter seasons (e.g., the beginning and end of the data). The data from the full year (February 1, 2019, to February 1, 2020) from periods when the corresponding reference concentrations were in the lowest quartile (e.g., $PM_{2.5} < 4.0 \ \mu g/m^3$, CO < 167 ppb, $O_3 < 22$, $NO_2 < 3$ ppb, NO < 0.2 ppb) was passed through the final calibration model with and without time as a predictor. The periods that fit these characteristics were spread

throughout the year. For example, of the qualifying O_3 hours, 20% of the hours came from the winter months, 21% came from the spring months, 25% came from the summer months, and 24% came from the autumn months. Ideally, baseline values would be assessed using periods when the concentration is equal to zero, but this is only possible in a laboratory setting. The average reference concentrations of $PM_{2.5}$, CO, O_3 , NO_2 , and NO during these periods were 2.4 μ g/m³, 148, 12.8, 2.3, and 0.1 ppb, respectively. For comparison, the reported limits of detection for $PM_{2.5}$, CO, O_3 , NO_2 , and NO are 1 μ g/m³, 20 ppb, 10 ppb, 1 ppb, and 1 ppb, respectively (see SI materials for further details).

3. RESULTS AND DISCUSSION

3.1. PM Sensor. The time series and scatterplots of the uncalibrated $PM_{2.5}$ sensor data from the training and the calibrated sensor data from the evaluation period are shown in

Table 2. Summary of the Predictors Used in the Regression Models Following the Structure of eq 1^a

	Predictors in Final Model								
PM _{2.5}	PM sensor*	T^\dagger	RH [†]	PM sensor—RH interaction	PM sensor—T interaction				
СО	CO sensor [†]	T^{\dagger}	CO sensor—T interaction	RH	RH-T interaction	time			
	CO sensor—time interaction								
NO ₂ (reference data)	NO ₂ sensor [†]	T	RH	NO ₂ sensor-RH interaction	reference O ₃	NO_2 sensor—reference O_3 interaction			
	reference NO	time							
NO ₂ (colocated sensors)	NO ₂ sensor [†]	T	RH	NO ₂ sensor—RH Interaction	O_3 sensor	NO ₂ sensor—O ₃ sensor interaction			
	O3 sensor $-T$ interaction	NO sensor	NO sensor—T interaction	time					
O ₃ (reference data)	O ₃ sensor [†] **	T^{\dagger}	O ₃ sensor—T interaction	RH^2	reference NO ₂	time			
O ₃ (colocated sensors)	O ₃ sensor [†] **	T^{\dagger}	O ₃ sensor—T interaction	RH^2	NO ₂ sensor	NO ₂ sensor—time interaction			
	NO sensor	NO sensor— T interaction	time						
NO (reference data)	NO sensor [†]	T^2	NO sensor— <i>T</i> interaction	reference CO	NO sensor—reference CO interaction				
NO (colocated sensors)	NO sensor [†]	T^2	NO sensor—T interaction	CO sensor	NO sensor—CO sensor interaction				

^aPredictors marked with † have been split into two coefficients at the median value. The predictor marked with * was split at 31 μ g/m³, and the predictor marked with * was split at 17 kΩ. Since the O₃, NO₂, and NO sensors exhibited cross sensitives to other common pollutants, we produced model iterations that used reference data from the colocated regulatory monitors or data from other sensors colocated in the monitor for comparison.

Figure 1A,B. The full-year time series of the uncalibrated and calibrated PM_{2.5} sensor data are shown in Figure S1. Overall, the uncalibrated Plantower PM_{2.5} sensor data exhibited a strong correlation with the reference instrument, but there were many periods where the mass concentration was overestimated, resulting in an RMSE of 9.2 and 8.6 μ g/m³ for the training and evaluation periods, respectively (Figures 1A, S1, Table 1). During the training period, the hourly averaged reference $PM_{2.5}$ mass concentration was 8.0 \pm 6.0 (average \pm one standard deviation) $\mu g/m^3$ (range: 0.10-44.0 $\mu g/m^3$), the uncalibrated sensor mass concentration was 12.7 \pm 12.3 μ g/m³, and the Pearson correlation coefficient (r) was 0.84 (Table 1). During the evaluation period, the average reference PM_{2.5} mass concentration was 8.8 \pm 6.0 μ g/m³ (range: $0.10-47.50 \mu g/m^3$), the uncalibrated sensor mass concentration was 12.4 \pm 11.7 μ g/m³, and the corresponding r value was 0.80. For comparison, the annual primary standard is 12.0 μ g/m³, and the 24 h standard is 35 μ g/m³.

The PM sensor was significantly impacted by both RH and temperature (p < 0.001; Table 2), and the uncalibrated sensor response, temperature, and RH values were the only parameters needed to calculate the final concentrations (Table 2). Introducing a spline into the sensor values (knot at 31 μ g/m³) resulted in the best model, and the calibration was improved by including the interaction terms for RH and temperature with the sensor. The model was further improved by including spline at the median temperature and RH values. An example of the predictors used in the regression models following the structure of eq 1 is shown in eq 4, where S_{low} , S_{high} , R_{low} , R_{high} , T_{low} , and T_{high} are binary indicator variables. The indicator variables will be set to either zero or one, so only the applicable predictor would be used for a given time (e.g., when the PM sensor value is below 31 μ g/m³, S_{low} and S_{high} would be one and zero, respectively). Please note the

numerical values may not be universally transferable, and the betas should be derived with data for each sensor.

$$\begin{aligned} \text{Reference PM}_{2.5}(t) &= -0.49 + 0.67^*\text{PM2.5}_{\text{sensor}}(t) \\ &*S_{\text{low}} + 0.92^*\text{PM2.5}_{\text{sensor}}(t) \\ &*S_{\text{high}} + 0.06^*\text{RH}_{\text{sensor}}(t)^*R_{\text{low}} \\ &- 0.03^*\text{RH}_{\text{sensor}}(t)^*R_{\text{high}} \\ &- 0.03^*\text{temperature}_{\text{sensor}}(t)^*T_{\text{low}} \\ &+ 0.26^*\text{temperature}_{\text{sensor}}(t)^*T_{\text{high}} \\ &- 0.004^*\text{PM2.5}_{\text{sensor}}(t)^*\text{RH}_{\text{sensor}}(t) \\ &- 0.001^*\text{PM2.5}_{\text{sensor}}(t) \end{aligned}$$

Over the year, the ambient temperatures ranged between -10 and 37 °C, and the ambient RH ranged between 14 and 96%. The PM sensor markedly overestimated the concentrations at a higher RH (e.g., >70%; Figure S1B) and, to a lesser extent, at a low temperature (e.g., <5 °C; Figure S1A). There was also a slight underestimation at low RH (<30%). These trends were observed for both higher (PM_{2.5} > 30 μ g/ m³) and lower (PM_{2.5} < 5 μ g/m³) mass concentrations. To visualize how the low-cost sensors responded to a given parameter, the sensor values were plotted as a function of temperature and RH in Figure S1. Optical PM sensors are known to overestimate mass concentrations at higher RHs due to the uptake of water on the surface of PM, so the overestimated concentration at high RH is likely due to physical changes of the particles themselves instead of the sensor responding to changes in RH directly. 12,33,34 Since PM_{2.5} is comprised of a broad range of compounds, it is possible that compositional differences between seasons, rather than actual temperature variations, produce the temperature

dependence, but without speciated PM data, this could not be evaluated further. 35,36

An evaluation was completed to determine if the PM sensor exhibited a sensor baseline drift over the full-year period. Lowcost PM sensors may exhibit drift due to aging of the electrical components or PM accumulating within the sensor itself.³⁶ Taking temperature and RH into consideration, the PM_{2.5} sensor did not exhibit a significant drift (Table S2). When time was included in the model, the time coefficient was very small <0.01 $(\mu g/m^3)$ /day and not significant (p > 0.05), and the RMSE was not improved by incorporating time. The calibration model applied to the training period produced an RMSE of 2.8 μ g/m³ and an r of 0.89 (Figure 1E, Table 1). After the MLR was employed to calibrate the out of sample sensor data (evaluation period), the averaged calibrated sensor concentration was $8.0 \pm 5.0 \,\mu\text{g/m}^3$, which corresponded to an RMSE of 3.4 μ g/m³, an r of 0.85, and a percent bias of -10.6%. The required accuracies of reference federal equivalency methods are that the linear regression must have a slope of 1 ± 0.1 , a y-intercept of $0 \pm 5 \mu g/m^3$, $r \ge 0.97$, and a percent bias within $\pm 10\%$ (40 CFR part 53, subpart C, Table C-4; 40 CFR part 58). The recommended performance metrics for PM_{2.5} air sensors are a slope of 1.0 \pm 0.35, an intercept of $-5 \le b \le 5 \mu g/m^3$, an r^2 of ≥ 0.70 (r = 0.83), and an RMSE $\le 7 \mu g/m^3$.

The Plantower sensor is becoming increasingly popular due to the stability of the sensor, its consistent accuracy (when calibrated), and compact size. 12,19,33,35,36,40-45 Several assessments have been conducted using low-cost light scattering particle monitors to evaluate their performances in different environments, so the biases of this measurement method due to RH, temperature, and particle composition are reasonably characterized. 4,12,34,35,46-49 Several previous studies have employed MLR to correct Plantower data. 50-54 RH and temperature were included in all the models in the previous studies. Other predictors that were found to be significant in a previous study were daytime (binary), weekend/weekday (binary), operating time (time and since installation), and sensor uptime (time since the last boot-up). 50-54 Many models only included the sensor output, RH, and temperature as predictors (without an interaction term or splines), but if only these predictors were included for our dataset, the RMSE during the evaluation period would increase to 5.24 μ g/m³, and the r would be 0.83. Recent work has shown that Plantower's "atmospheric environment" CF produces a nonlinear shift in PM_{2.5} over 30 μ g/m³ (relative to CF = 1), and we suspect that our model's spline with a knot at 31 μ g/m³ accommodates this change in the relationship. Thus, future deployments may use the "CF = 1" settings to reach a similar result and better performance without the requisite spline/ knot. 55,56 It has been shown that the bias may vary as a function of the hour of the day, so including this as a predictor may further improve the model RMSE (e.g., including a CF for each hour of the day). 52 For example, an analysis completed at the same site as this study found that this Plantower sensor was more likely to underestimate the PM concentration overnight around midnight and overestimate the PM concentration during the day even after the data were corrected for RH and temperature biases.⁵² However, this is likely due to changing PM composition and not an intrinsic sensor bias for a given hour. Compared to other low-cost sensors, the Plantower generally exhibited comparable or higher correlations with reference data and low limits of detection. 12,35,43,57 Given the

rapid development of PM sensors over the last few years, few other studies have been able to assess the long-term performance of the sensor. The manufacturer reports a lifetime of greater than 3 years, and a study that deployed four Plantower sensors (though a previous sensor model) over 2 years reported that three out of the four sensors were working correctly at the end of the study. The sensors were working correctly at the end of the study.

3.2. CO Sensor. The time series of the uncalibrated CO sensor data from the training and the calibrated sensor data from the evaluation period are shown in Figure 1C,D along with scatterplots, and the complete time series of both the uncalibrated and calibrated sensor data are shown in Figure S2. The uncalibrated CO sensor signal responds similarly to the reference CO (Table 1; Figure 1C). Periods of high and low values corresponded, but the magnitude of the uncalibrated responses did not always align with that of the reference instrument. During the training period, the hourly averaged reference CO concentration was 234 ± 144 ppb (range: 113– 1756 ppb), and the corresponding r value with the uncalibrated sensor response was 0.51 (Figure 1F, Table 1). We note that the raw sensor values shown in Figure 1 are not representative or transferable across all CO sensors of the same model. This also applies to the other gas sensor signals discussed below and highlights the importance of sensor QA/ QC and calibration since sensors from the same batch may inherently produce different baseline values or pollutant response factors, though they will generally show similar responses to pollutants or environmental conditions.⁵⁹ During the evaluation period, the average reference CO concentration was 282 ± 248 ppb. The reference concentration during the evaluation period ranged between 103 and 2947 ppb. For comparison, the 1 h standard for CO is 35 ppm.³⁸ The regulatory monitoring requirements for CO instruments are precision and bias errors within 10%.60

The uncalibrated sensor voltage, temperature, RH, and time parameters were used in the final model (Table 2). Separating the sensor voltage and the temperature into two predictors at the median and including interaction terms for time with the sensor, temperature with the sensor, and RH with temperature resulted in the best calibration model. To visualize how the sensor responded to the environmental conditions, the sensor values were plotted as a function of temperature and RH in Figure S2. The CO sensor responded strongly to temperature and modestly to RH. The response of the sensor was relatively consistent between −10 and 15 °C, suggesting that lower temperatures may not bias the results considerably (Figure S2A). As the temperature increased above 20 °C, the CO sensor exhibited an increasing response with increasing temperature. These trends were observed at both higher and lower reference CO concentrations. Low-cost electrochemical sensors such as this one may respond strongly to environmental conditions because the electrochemical reactions that are used to determine the concentration may be influenced by temperature or RH.61 While the overall dependence on RH was minor, including this predictor notably increased the accuracy of the peak wintertime periods (Figure S2B). When NO was included as a predictor, it was significant and improved model accuracy, but this was likely because the reference NO and CO values exhibited a strong correlation (r = 0.83, Table S1), potentially due to coemissions from combustion-related sources in the region. Furthermore, NO has been previously reported to not be an interferant for this sensor.62

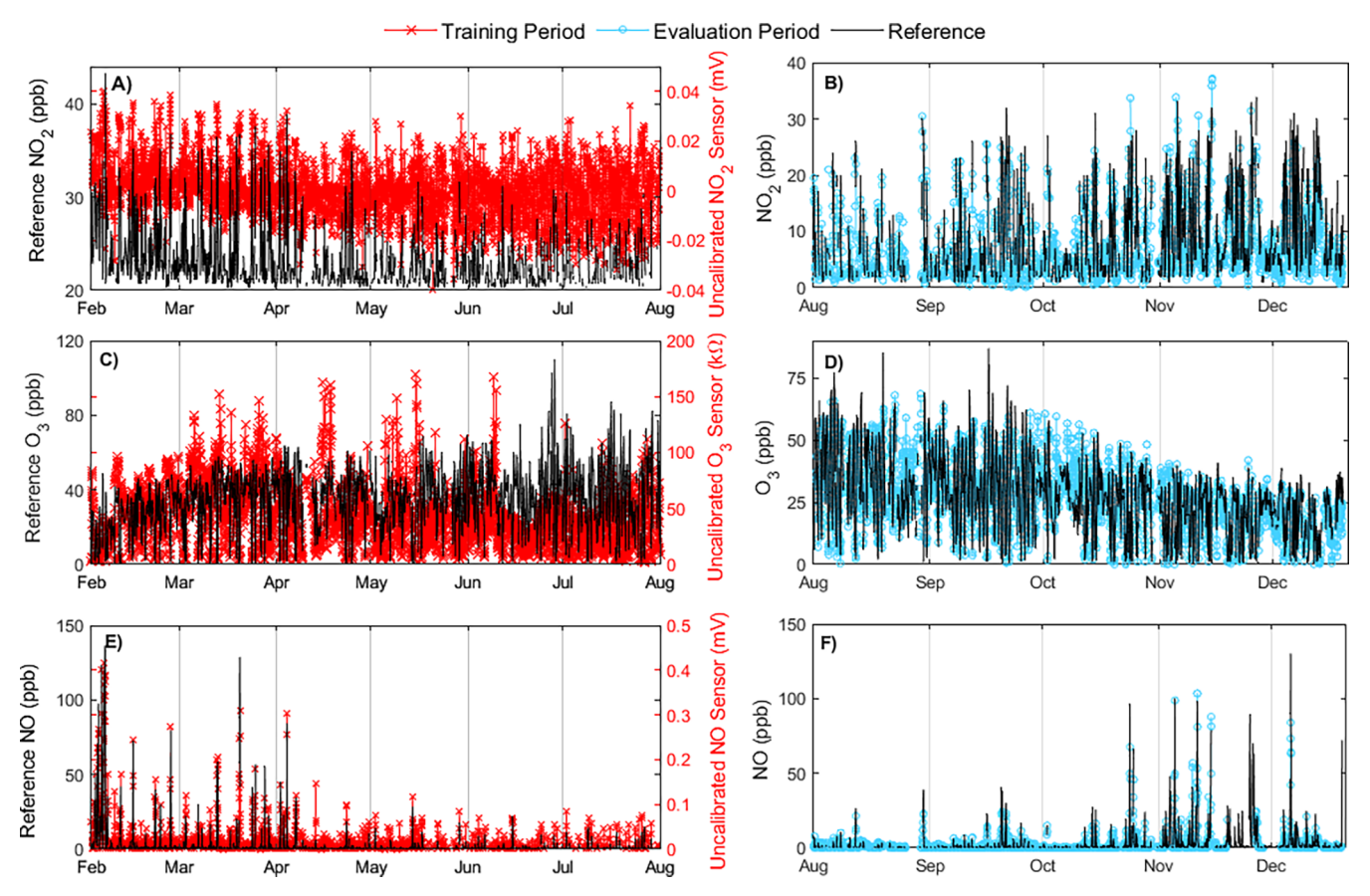


Figure 2. Time series of the hourly averaged reference data (black) and NO_2 , O_3 , and NO sensor data from the training (uncalibrated data shown in red; left column) and evaluation (calibrated shown in blue; right column) periods. The uncorrected NO_2 and NO sensors (in mV) are the difference between the working electrode and the auxiliary electrode.

When evaluating CO sensor baseline drift over the full-year period, the CO sensor did exhibit a significant drift (Table S2). When time and its interaction term with sensor voltage were included in the model, the RMSE from the evaluation period was improved by 44.8 ppb. After the MLR was applied to the evaluation data, the averaged calibrated sensor concentration was 297 ± 238 ppb, which corresponds to an RMSE of 58.9 ppb, an r value of 0.97, and a percent bias of 5.6% (Figure 2F, Table 1). The calibration model applied to the training period produced an RMSE of 60.5 ppb and an r of 0.90.

The CO-A4 sensor has been used in a variety of locations, including ambient, indoors, and industrial settings. 18,48,62-64 The CO sensor exhibited good correlations in all the environments (>0.58), and the RMSE varied between about 32-212 ppb, depending on observed concentrations and averaging time of the sensor. 9,18,48,62 The highest RMSE was observed in the region with the highest concentrations (average: 575 ppb over 19 days in China), but this was reported for a 1 min interval. 48 Castell et al. reported an RMSE of 170.99 ppb for 15 min-averaged CO data. 62 Our field results were similar to a lab-based study assessing the sensor response to changing environmental conditions. In that study, a comparable sensor (CO-B4) was exposed to a wide range of environmental conditions in control laboratory conditions (6 RH levels from 10 to 85% with increasing steps of 15% and four temperature levels of 10, 25, 35, and 45 °C).65 The authors also noted that the sensor responded to both RH and temperature, and the temperature response was not linear at higher temperatures.

3.3. NO₂ **Sensor.** The time series of the uncalibrated NO₂ sensor data from the training and the calibrated sensor data from the evaluation period are shown in Figure 2A,B, and the full-year time series of the uncalibrated and calibrated NO₂ sensor data are shown in Figure S3. During the training period, the hourly averaged reference NO₂ concentration was 7.9 \pm 7.9 ppb, and the corresponding r value with the uncalibrated sensor response was 0.71 (Figure 2, Table 1). The reference concentration ranged between 0 and 57.5 ppb. During the evaluation period, the average reference NO₂ concentration was 8.1 \pm 7.0 ppb, which ranged between 0 and 38 ppb. The 1 h standard for NO₂ is 100 ppb, and the annual standard is 53 ppb. The regulatory monitoring requirements for NO₂ instruments are precision and bias errors within 15%.

The final calibration models included the uncalibrated sensor response, temperature, RH, O₃, NO, and time parameters (Table 2). Separating the sensor into two predictors at the median and including interaction terms for RH and O₃ with the sensor resulted in the best model. If NO and O₃ are excluded from the model, the model RMSE from the reference predictor model increases by about 1.6 ppb (compared to 3.3 ppb). If NO is excluded, the model RMSE increases by 0.2 ppb, and if O₃ is excluded, the model RMSE increases by 1.0 ppb. Excluding O₃ as a predictor resulted in consistently overestimated daytime NO₂ concentrations. When NO was removed from the model, the peak values were consistently underestimated during the winter months. To visualize how the sensor responded to these predictors, the sensor values were plotted as a function of temperature and

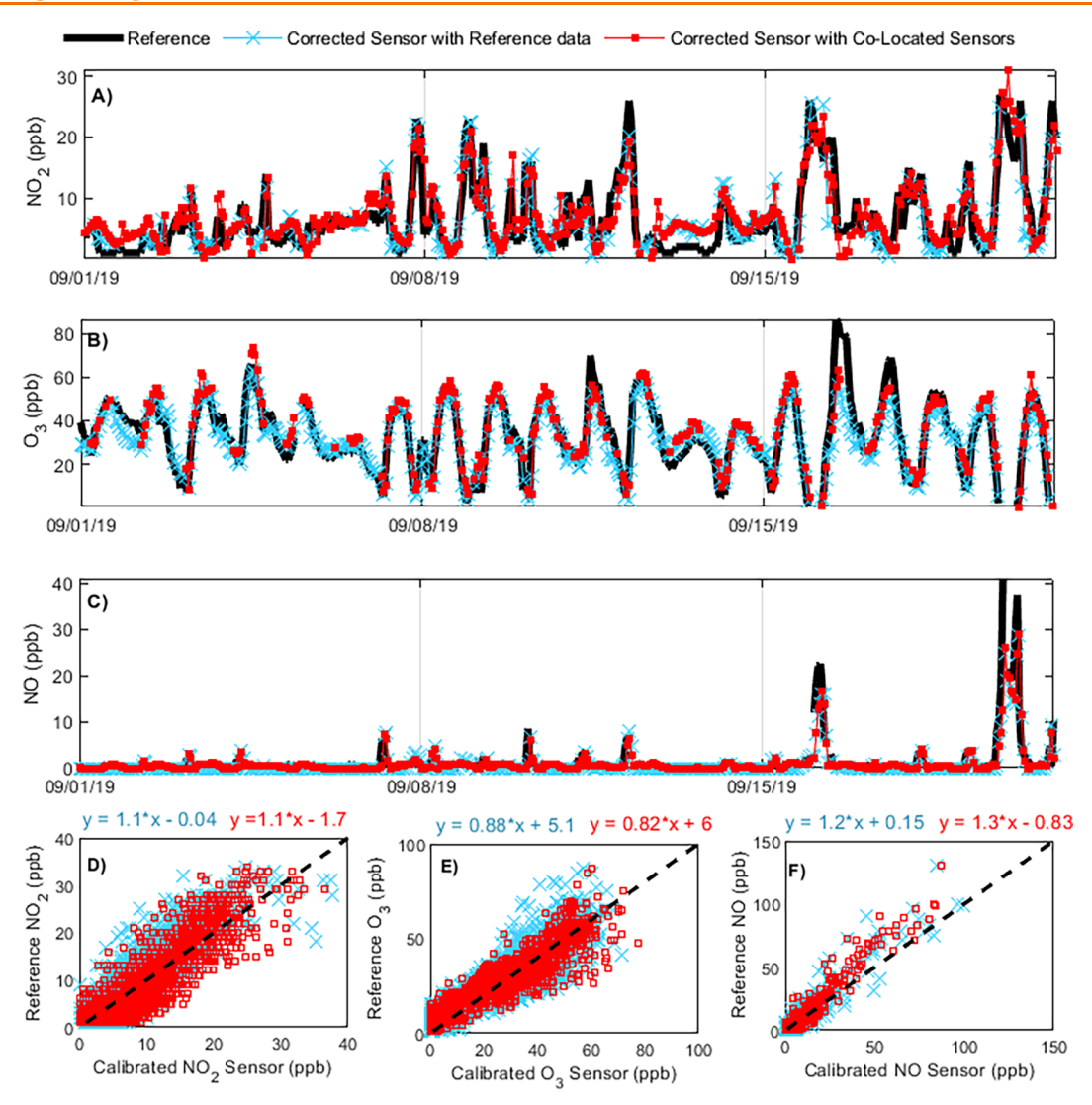


Figure 3. Calibration model results using either hourly reference data or colocated sensors as predictors to correct from cross-sensitive pollutants for (A) O_3 , (B) NO_2 , and (C) NO sensors, shown in greater detail for September 2019. The blue line was calculated using reference data for the predictors needed in the model (same as in Figure 2), and the red line was calculated by using data from other sensors colocated in the box. (D–F) Scatterplots of the model results and the reference data from the full evaluation period. The linear fits for the evaluation periods are displayed.

RH in Figure S3. The most influential predictors, excluding the sensor itself, were O_3 and NO concentrations, and temperature and RH were significant but minor predictors. When evaluating the NO_2 sensor for baseline drift and accounting for the other predictors, the NO_2 sensor exhibited a drift of less than 0.01 ppb/day (p = 0.03; Table S2). When time was included in the model, the RMSE from the evaluation period was improved by about 0.3 ppb.

Since the NO_2 sensor responded to interferant gases, two models were evaluated: one with the colocated reference data as predictors and one with the colocated raw sensor responses as predictors. The colocated sensor model used two additional predictors (the O_3 -temperature and NO-temperature interaction term) to account for the response to temperature by the O_3 and NO sensors. Overall, the models with the colocated reference data performed slightly better than with the colocated sensors, but the differences between the RMSE were small (0.3 ppb during the training period and 0.1 ppb during the evaluation period). After the MLR models were used to calibrate the evaluation period, the averaged calibrated sensor concentration was 7.8 ± 5.7 ppb (RMSE of 3.5 ppb; r =

0.88; percent bias = -9.0%) for the calibration model with colocated reference data and 9.4 ± 5.8 (RMSE of 3.6 ppb; r = 0.88; percent bias = 11.5%) for the calibration model with colocated sensor O_3 measurements. The MLR applied to the training period produced an RMSE of 3.3 ppb (reference model) and 3.6 ppb (sensor model) and similar r values (r = 0.91 and 0.90, respectively; Figure 3D). The time series of the sensor data calibrated using the two different models from September 2019 are shown in Figure 3A. Overall, both calibration models appear to reproduce the diurnal trends on almost all days.

In comparison with other field deployments using this sensor, we observed comparable or better correlations in our study [e.g., r = 0.83 (5 min), 18 0.88 (10 min), 11 <0.7 (15 min), 62 and 0.79 (1 h), 66 but since the reported time intervals ranged between 5 min and 1 h, it can be difficult to directly compare with our study. The corresponding RMSE were 4.56, 8.3, 30.27 ppb, and not reported, respectively, in those studies. For comparison, Bigi et al. compared the potential RMSE and r^2 using MLR (predictors included T, RH, NO₂, and NO), support vector regression, and random forest using a data set

comprised of 4 months of training and 4 months of the deployment at an urban, heavily trafficked site. 11 They reported 10 min RMSE of 5.5, 4.6, and 4.4 ppb, respectively, and they were able to better characterize the full concentration range using the nonlinear methods. In another laboratory study, when a similar sensor (NO₂-B4) was tested in a wide range of environmental conditions as described above, the sensor was found to be sensitive to RH above about 55%. For lower RHs, the signal was stable, but as the RH increased, the signal become nosier and overestimated the concentration. They reported that the sensor responded strongly to high temperatures (>45 $^{\circ}$ C), and the signal decreased with increasing temperatures.

We found that O_3 was a significant predictor. The sensor is designed to filter out O_3 before measuring NO_2 , and the filter is rated to withstand 500 hr at 2 ppm. When the sensors were evaluated prior to deployment in January 2019 in chamber testing, the NO_2 sensor did not exhibit a response to O_3 . It has also been shown that as the NO_2 sensor ages, the built-in O_3 scrubber can degrade, resulting in an increasing crosssensitivity to O_3 and reduced sensor accuracy, and others have seen variations in the efficacy of the ozone scrubber, including ozone breakthrough and filter aging. 10,67 Thus, we considered in our model the possibility of continued crosssensitivity of the NO_2 sensor to ozone.

While we did not observe substantial deterioration in NO_2 sensor performance over the evaluation period, the NO_2 sensor performance should be continually evaluated. Castell et al. reported that their NO_2 sensor did not exhibit a cross-sensitivity to O_3 , whereas van Zoest et al. included O_3 in their MLR since it reduced the overall RMSE (predictors were NO_2 , O_3 , RH, T, wind speed, and wind direction). Several other field deployments have reported a minor sensor drift after only a few months. 11,70

3.4. O_3 **Sensor.** The time series of the uncalibrated O_3 sensor data from the training are shown with the calibrated sensor data from the evaluation period in Figure 2C,D, while the full annual time series of the uncalibrated and calibrated O₃ sensor data are shown in Figure S4. During the training period, the hourly averaged reference O_3 concentration was 35.5 \pm 15.7 ppb, and the corresponding r value was 0.52 (Figure 2, Table 1). The reference concentration ranged between 0 and 106.5 ppb. During the evaluation period, the hourly averaged reference O_3 concentration was 28.5 \pm 14.9 ppb, and the corresponding r value of the uncalibrated sensor response was 0.52. The 8 h standard for O₃ is 70 ppb.³⁸ The regulatory monitoring requirements for an O₃ instrument are precision and bias errors within 7%. The recommended performance metrics for O_3 air sensors are a slope of 1.0 ± 0.2 , an intercept of $-5 \le b \le 5$ ppb, an r^2 of ≥ 0.80 (r = 0.89), and an RMSE \le 5 ppb.

The final calibration models included the uncalibrated sensor values, temperature, RH, NO₂, and time predictors (Table 2). Separating the sensor into two predictors and including interaction terms for temperature with the sensor resulted in the best model. The sensor exhibits a much higher slope below about 17 k Ω and then remains generally flat (Figure S4G), so this was where the knot was placed. If NO₂ was excluded, the colocated reference model RMSE increases by 0.7 ppb (compared to 6.9 ppb). The O₃ sensor exhibited the strongest responses to temperature, followed by NO₂ and then RH. The output of the sensor notably decreases as the temperature increases, which resulted in underestimating the

true O₃ concentration at high temperatures (Figure 3B). A concentration of about 35 ppb corresponded to an average value of about 780 k Ω at 0 °C compared to about 162 k Ω at 40 °C (Figure S5). It is important to note when using this sensor that high temperatures and high ozone concentrations often coexist, which can result in the sensor values exhibiting little change during increasing O₃ concentrations or even decreasing values, driven by the change in temperature, not O₃ concentration. When the uncalibrated O₃ sensor is plotted as a function of RH or NO2, the visual trend suggests that O3 would be overestimated at lower values (Figure S4), but after the temperature was taken into consideration, exposure to increasing NO₂ and RH results in overestimating the O₃ concentration. An evaluation was completed to determine if the O₃ sensor exhibited a sensor baseline drift over the full-year period. After accounting for the other predictors, the O₃ sensor exhibited a drift of about -0.01 ppb/day using the colocated reference model (p = 0.03; Table S2). When time was included in the reference model, the RMSE from the evaluation period was improved by 1.6 ppb.

Since the sensor responded to an interferant gas, models with the colocated reference and colocated sensor data as predictors were evaluated. The colocated sensor model required additional predictors to correct for biases from the raw NO2 sensor data, so the colocated raw NO sensor response, the NO₂-time interaction, and NO-temperature interaction terms were also included. Overall, the models performed similarly. The differences between the RMSE were small during the training period (the reference model RMSE was better by 0.2 ppb) and evaluation periods (the colocated sensor model RMSE was better by 0.4 ppb). After the MLR models were used to calibrate the evaluation period, the averaged calibrated sensor concentration was 28.4 ± 13.6 (RMSE of 7.4 ppb; r = 0.86; percent bias = -7.1%) for the colocated reference model and 28.3 ± 15.5 (RMSE of 7.0 ppb; r = 0.89; percent bias = -4.0%) for the colocated sensor model. The MLR applied to the training period produced a similar RMSE (reference model = 6.9 ppb; sensor model = 7.1 ppb) and r values (r = 0.90 and 0.90, respectively). The time series of the calibrated sensor data using the two different models from September 2019 are shown in Figure 3B. On many of the evaluation days, the calibrated sensor reproduced the temporal trends and concentrations, but both models significantly underestimated the ozone concentration on the day exhibiting the greatest concentration (e.g., September 16, 2019). Even if the model was refit to consider only August data in the training period and the month of September as the evaluation period, the model was unable to reproduce the peak concentration on September 16th. To examine this further, if we average the time points when the reference O₃ was greater than 70 ppb, the average reference concentration was 78.2 ppb compared to 57.7 for the colocated reference model and 61.9 for the colocated sensor calibration model. The sensor also frequently overestimated the lower concentrations (Figure 3E). If we average the time points when the reference O_3 was less than 20 ppb, the average reference concentration is 10.5 ppb compared to 15.6 for the colocated reference model and 10.1 for the colocated sensor model.

Ripoll et al. colocated 132 metal-oxide MICS 2614 (apportioned into 44 sensing devices) at reference stations in Italy (4 stations) and Spain (5 stations) for 5 months (May–October).⁷¹ They reported a mean hourly averaged r^2 of 0.88 (r = 0.94) and RMSEs between 4.5 and 13 ppb. Similar to our

data, the sensors were not able to capture the highest concentrations and exhibited an upper limit of about 85 ppb. When the authors tried to calibrate the data using MLR with the raw sensor output, temperature, and RH as coefficients, they were unable to capture the peak concentrations; however, a subset analysis indicated that nonlinear methods, such as support vector regression, were more promising. They did not observe sensor drift during the 5 month deployment. Buehler et al. observed a similar negative temperature dependence in the ozone sensor with temperature over a more narrow temperature and ozone concentration range.9 When MICS-2614 sensors were worn by 8 volunteers in Texas during the daytime on the weekdays and weekends between January to March, the sensors performed best for concentrations between 20 and 100 ppb. 72 The O3 MICS-2614 has been less commonly used than the AlphaSense Ox sensors in urban applications. The two sensors can both yield useable data, but they have different limitations. The Ox sensors exhibit a higher NO₂ dependency and lower correlations but exhibit reasonable measurements at higher concentrations. 18,36,71,73 They also exhibit a temperature dependence, but it increased the output (similar to the CO sensor), which makes it less of an issue than with the MICS sensor. The inability of this sensor to capture peak concentrations during warm seasons may limit their use in health-related research.

3.5. NO Sensor. The uncalibrated NO sensor data from the training and the calibrated sensor data from the evaluation period are shown in Figure 2E,F, with the full data shown in Figure S6. During the training period, the hourly averaged reference NO concentration was 3.0 ± 11.0 ppb (Table 1), which ranged widely between 0 and 134 ppb. During the evaluation period, the average reference NO concentration was 3.3 ± 10.0 ppb (Table 1). The reference concentration during the evaluation period ranged between 0 and 130 ppb.

The final calibration models included the uncalibrated sensor output, temperature, CO, and time predictors (Table 2). Separating the sensor into two predictors at the median and including interaction terms for temperature and CO with the sensor resulted in the best model. RH was not significant and did not improve the model. The response of the sensor was relatively consistent below 20 °C, suggesting that lower temperature may not bias the results considerably (Figure S6C), and the sensor output decreased as the temperature increased above about 20 °C. These trends were observed at both higher and lower reference NO concentrations. Overall, the sensor appeared to underestimate the true concentration during periods of higher CO concentrations, and including the reference CO concentration as a predictor in the colocated reference model improved the RMSE by 0.79 ppb. The improvement was more pronounced during periods of peak NO concentrations. When evaluating sensor baseline drift over the full-year period, the time coefficient (included in the model) was very small <0.01 ($\mu g/m^3$)/day and not significant, and RMSE was not improved by incorporating time (Table S2).

The calibration models with the colocated reference and colocated uncalibrated sensor data as predictors were evaluated to correct for cross-sensitivities to other gases. The time series of the sensor data calibrated using the two different models from September 2019 are shown in Figure 3C. Overall, the models performed similarly, and the differences between the RMSE were small during the training period (the reference model RMSE was better by 0.4 ppb) and evaluation periods

(the colocated sensor model RMSE was better by 0.1 ppb). After the colocated reference model was applied to the evaluation data, the averaged calibrated sensor concentration was 2.8 ± 8.3 ppb, with an RMSE of 3.3 ppb, an r value of 0.96, and a percent bias of -14.7% (Figure 3F). The higher RMSE is driven by the underestimation of the peak NO values, but 73% of the reference model hours were within ± 1 ppb. The reference model applied to the training period produced an RMSE of 3.0 ppb and an r of 0.96. After the colocated sensor model was applied to the evaluation data, the averaged calibrated sensor concentration was 3.3 ± 7.8 ppb, with an RMSE of 3.2 ppb, an r value of 0.97, and a percent bias of -2.7%. The colocated model applied to the training period produced an RMSE of 3.4 ppb and an r of 0.95. Overall, the models reproduced the diurnal trends, but peak exposures were sometimes underestimated.

We observed comparable correlations in our study to those previously reported (e.g., r = 0.92 (5 min), 18 0.97 (10 min) 11 in those studies). The corresponding RMSE from those studies were 4.52 and 3.54, respectively. Bigi et al. also compared the RMSE and r² of NO using MLR (predictors included T, RH, NO₂, and NO), support vector regression, and random forest.¹¹ The reported 10 min RMSE were 8.3, 7.1, and 7.1 ppb, respectively. Interestingly, even the nonlinear models were not able to reproduce all of the peaks on the most polluted days. 11 The underestimation of peak NO concentrations was also observed in other field studies. 18 When the similar NO-B4 sensor was exposed to a range of six RH levels and four temperatures in laboratory conditions, the sensor did not exhibit a consistent trend with increasing RH.65 They reported that the sensor responded strongly to increasing temperatures. We note that we used the difference between the working electrode and the auxiliary electrode for NO, NO₂, and CO to leverage the initial (partial) temperature correction afforded by AlphaSense's auxiliary electrode but show in Figures S2, S3, and S6 that it is insufficient to overcome the temperature effect, which is similarly shown by Cross et al. and Tryner et al. 18,56 While our calibration model corrects for the temperature influences, we note that future iterations should test performance without the auxiliary electrode, especially at a higher time resolution (<1 h), where lags in these responses to temperature may introduce further deviations. A few studies have reported a minor sensor drift, but a 22 month study determined that the drift for the NO sensors was not statistically significant. 11,70,74

4. CONCLUSIONS

In this study, we assessed the colocated reference and low-cost sensor data sets for five pollutants (PM_{2.5}, CO, O₃, NO₂, and NO) using MLR models to calibrate the data to identify key parameters that need to be measured to develop accurate calibration equations for multipollutant network data (e.g., SEARCH). We also evaluated using colocated low-cost sensors to correct other sensors and how that compared to having the reference data for the cross-sensitivity. This study demonstrates that these low-cost sensors can characterize ambient urban pollution over longer periods of time. All of the sensor calibration models produced high Pearson correlation coefficients (r) at the hourly resolution, and the averages of the calibrated sensor and the reference data from the evaluation period were within 12%. The PM_{2.5}, CO, NO₂, O₃, and NO sensors were trained using 6 months of data collected over a wide range of temperature and RH conditions,

resulting in RMSE values of 3.4 μ g/m³, 58.9, 3.5, 7.4, and 3.3 ppb, respectively.

Each of the sensors required a distinct set of predictors to achieve the lowest possible RMSE. All of the sensors responded to environmental factors, such as temperature (all five sensors) or RH (PM_{2.5}, O₃, NO₂), and the O₃, NO₂, and NO sensors exhibited cross-sensitives to another air pollutant. The CO, O₃, and NO₂ sensors exhibited some baseline drift over the year, while the PM_{2.5} and NO sensors were more stable. The MLR models were generally able to characterize the diurnal trend and concentration ranges of the sensor, but nonlinear methods may be more appropriate for the ozone in warm environments. Since the NO and O₃ sensors are unable to capture peak concentrations during some environmental conditions, caution should be used in health-related research since short-term peak exposures can lead to a range of negative health effects and premature mortality.⁷⁵

One strength of deploying multipollutant monitors is that if the interferants are known, the sensor data may be calibrated with colocated sensors. This is particularly useful when correcting data collected at locations away from reference instruments, as is needed to improve the spatial resolution of measurements, or when the interfering gas is less frequently measured. This work was completed in a region that experiences a wide range of environmental conditions over a full year, which permitted us to assess the importance of each predictor and can inform future users what sensors need to be comeasured in other locations. We compared the RMSE from models that used the colocated reference and sensor data for the interferant gases. The O₃, NO₂, and NO colocated sensor models produced RMSE within 0.5 ppb of the calibration models utilizing reference data as predictors. This indicates that low-cost sensor networks should be able to yield accurate data if the monitoring package is designed to comeasure key predictors that can be used to correct a sensor for known biases (e.g., yield similar concentrations and diurnal patterns and all percent bias were within 15%). This is key for the utilization of low-cost sensors by diverse audiences since this does not require continual access to regulatory grade instruments or advanced machine learning approaches. We chose to use MLR models for these low-cost sensors because they may be more accessible to a wider range of sensor users, as opposed to more complex machine learning models. We also evaluated nonlinear components (i.e., quadratics and splines) in the model, which has not commonly been done in previous literature involving MLR and low-cost sensors. We found this improved model RMSE and still maintains the lower complexity of the MLR approach. Future work should focus on the transferability of calibration from one sensor unit to another unit and from one location to another.

ASSOCIATED CONTENT

Supporting Information

The Supporting Information is available free of charge at https://pubs.acs.org/doi/10.1021/acsestengg.1c00367.

Additional details on sensors used in this study, the final regression models, the correlations of the measured pollutant and environmental conditions, the baseline sensor values over the full year, and the uncalibrated and calibrated PM_{2.5}, CO, NO₂, O₃, NO data from the full year (PDF)

AUTHOR INFORMATION

Corresponding Author

Misti Levy Zamora — Department of Public Health Sciences UConn School of Medicine, University of Connecticut Health Center, Farmington, Connecticut 06032-1941, United States; Environmental Health and Engineering, Johns Hopkins University Bloomberg School of Public Health, Baltimore, Maryland 21205-2103, United States; SEARCH (Solutions for Energy, Air, Climate and Health) Center, Yale University, New Haven, Connecticut 06520, United States; orcid.org/0000-0002-4832-7753; Email: mzamora@UCHC.edu

Authors

Colby Buehler – SEARCH (Solutions for Energy, Air, Climate and Health) Center, Yale University, New Haven, Connecticut 06520, United States; Chemical and Environmental Engineering, Yale University, New Haven, Connecticut 06520, United States

Hao Lei – Environmental Health and Engineering, Johns Hopkins University Bloomberg School of Public Health, Baltimore, Maryland 21205-2103, United States

Abhirup Datta — Department of Biostatistics, Johns Hopkins University Bloomberg School of Public Health, Baltimore, Maryland 21205-2103, United States

Fulizi Xiong – SEARCH (Solutions for Energy, Air, Climate and Health) Center, Yale University, New Haven, Connecticut 06520, United States; Chemical and Environmental Engineering, Yale University, New Haven, Connecticut 06520, United States

Drew R. Gentner – SEARCH (Solutions for Energy, Air, Climate and Health) Center, Yale University, New Haven, Connecticut 06520, United States; Chemical and Environmental Engineering, Yale University, New Haven, Connecticut 06520, United States

Kirsten Koehler — Environmental Health and Engineering, Johns Hopkins University Bloomberg School of Public Health, Baltimore, Maryland 21205-2103, United States; SEARCH (Solutions for Energy, Air, Climate and Health) Center, Yale University, New Haven, Connecticut 06520, United States; orcid.org/0000-0002-0516-6945

Complete contact information is available at: https://pubs.acs.org/10.1021/acsestengg.1c00367

Notes

The authors declare no competing financial interest.

ACKNOWLEDGMENTS

This publication was developed under Assistance Agreement no. RD835871 awarded by the U.S. Environmental Protection Agency to Yale University. It has not been formally reviewed by the Environmental Protection Agency (EPA). The views expressed in this document are solely those of the authors and do not necessarily reflect those of the Agency. The EPA does not endorse any products or commercial services mentioned in this publication. The authors thank the Maryland Department of the Environment Air and Radiation Management Administration for allowing us to collocate our sensors with their instruments at the downtown Baltimore site. M.L.Z. is supported by the National Institute of Environmental Health Sciences of the National Institutes of Health under awards number K99ES029116. The content is solely the responsibility of the authors and does not necessarily represent the official

views of the National Institutes of Health. F.X. and D.R.G. would also like to acknowledge support from HKF Technology (a Kindwell company). A.D. is supported by the National Science Foundation DMS-1915803 and the National Institute of Environmental Health Sciences (NIEHS) grant R01ES033739. C.B. is supported by the National Science Foundation Graduate Research Fellowship Program under grant no. DGE1752134. Any opinions, findings, conclusions, or recommendations expressed in this material are those of the author(s) and do not necessarily reflect the views of the National Science Foundation.

REFERENCES

- (1) Tan, B. Laboratory Evaluation of Low to Medium Cost Particle Sensors. MS Thesis, University of Waterloo, 2017.
- (2) Ikram, J.; Tahir, A.; Kazmi, H.; Khan, Z.; Javed, R.; Masood, U. View: implementing low cost air quality monitoring solution for urban areas. *Environ. Syst. Res.* **2012**, *1*, 10.
- (3) Mead, M. I.; Popoola, O. A. M.; Stewart, G. B.; Landshoff, P.; Calleja, M.; Hayes, M.; Baldovi, J. J.; McLeod, M. W.; Hodgson, T. F.; Dicks, J.; Lewis, A.; Cohen, J.; Baron, R.; Saffell, J. R.; Jones, R. L. The use of electrochemical sensors for monitoring urban air quality in lowcost, high-density networks. *Atmos. Environ.* **2013**, *70*, 186–203.
- (4) Sousan, S.; Koehler, K.; Thomas, G.; Park, J. H.; Hillman, M.; Halterman, A.; Peters, T. M. Inter-comparison of low-cost sensors for measuring the mass concentration of occupational aerosols. *Aerosol Sci. Technol.* **2016**, *50*, 462–473.
- (5) Clements, A. L.; Griswold, W. G.; Rs, A.; Johnston, J. E.; Herting, M. M.; Thorson, J.; Collier-Oxandale, A.; Hannigan, M. Low-cost air quality monitoring tools: from research to practice (a workshop summary). *Sensors* **2017**, *17*, 2478.
- (6) Bart, M.; Williams, D. E.; Ainslie, B.; McKendry, I.; Salmond, J.; Grange, S. K.; Alavi-Shoshtari, M.; Steyn, D.; Henshaw, G. S. High Density Ozone Monitoring Using Gas Sensitive Semi-Conductor Sensors in the Lower Fraser Valley, British Columbia. *Environ. Sci. Technol.* **2014**, *48*, 3970–3977.
- (7) Snyder, E. G.; Watkins, T. H.; Solomon, P. A.; Thoma, E. D.; Williams, R. W.; Hagler, G. S.; Shelow, D.; Hindin, D. A.; Kilaru, V. J.; Preuss, P. W. The Changing Paradigm of Air Pollution Monitoring. *Environ. Sci. Technol.* **2013**, 47, 11369–11377.
- (8) Hagler, G. S.; Williams, R.; Papapostolou, V.; Polidori, A. Air Quality Sensors and Data Adjustment Algorithms: When Is it No Longer a Measurement? *Environ. Sci. Technol.* **2018**, *52*, *5530*–*5531*.
- (9) Buehler, C.; Xiong, F.; Zamora, M. L.; Skog, K. M.; Kohrman-Glaser, J.; Colton, S.; McNamara, M.; Ryan, K.; Redlich, C.; Bartos, M.; Wong, B.; Kerkez, B.; Koehler, K.; Gentner, D. R. Stationary and portable multipollutant monitors for high-spatiotemporal-resolution air quality studies including online calibration. *Atmos. Meas. Tech.* **2021**, *14*, 995–1013.
- (10) Li, J.; Hauryliuk, A.; Malings, C.; Eilenberg, S. R.; Subramanian, R.; Presto, A. A. Characterizing the Aging of Alphasense NO2 Sensors in Long-Term Field Deployments. *ACS Sens.* **2021**, *6*, 2952–2959.
- (11) Bigi, A.; Mueller, M.; Grange, S. K.; Ghermandi, G.; Hueglin, C. Performance of NO, NO2 low cost sensors and three calibration approaches within a real world application. *Atmos. Meas. Tech.* **2018**, 11, 3717–3735.
- (12) Levy Zamora, M.; Xiong, F.; Gentner, D.; Kerkez, B.; Kohrman-Glaser, J.; Koehler, K. Field and Laboratory Evaluations of the Low-Cost Plantower Particulate Matter Sensor. *Environ. Sci. Technol.* **2019**, *53*, 838–849.
- (13) Schneider, P.; Bartonova, A.; Castell, N.; Dauge, F. R.; Gerboles, M.; Hagler, G. S. W.; Hüglin, C.; Jones, R. L.; Khan, S.; Lewis, A. C.; Mijling, B.; Müller, M.; Penza, M.; Spinelle, L.; Stacey, B.; Vogt, M.; Wesseling, J.; Williams, R. W. Toward a Unified Terminology of Processing Levels for Low-Cost Air-Quality Sensors. *Environ. Sci. Technol.* **2019**, *53*, 8485–8487.

- (14) Arnaudo, E.; Farasin, A.; Rossi, C. A Comparative Analysis for Air Quality Estimation from Traffic and Meteorological Data. *Appl. Sci.* **2020**, *10*, 4587.
- (15) Rybarczyk, Y.; Zalakeviciute, R. Machine learning approaches for outdoor air quality modelling: A systematic review. *Appl. Sci.* **2018**, *8*, 2570.
- (16) Zimmerman, N.; Presto, A. A.; Kumar, S. P. N.; Gu, J.; Hauryliuk, A.; Robinson, E. S.; Robinson, A. L.; Subramanian, R. A machine learning calibration model using random forests to improve sensor performance for lower-cost air quality monitoring. *Atmos. Meas. Tech.* **2018**, *11*, 291.
- (17) Taylor, M. D. In Low-cost air quality monitors: Modeling and characterization of sensor drift in optical particle counters. 2016 IEEE Sensors; IEEE, 2016; pp 1–3.
- (18) Cross, E. S.; Williams, L. R.; Lewis, D. K.; Magoon, G. R.; Onasch, T. B.; Kaminsky, M. L.; Worsnop, D. R.; Jayne, J. T. Use of electrochemical sensors for measurement of air pollution: Correcting interference response and validating measurements. *Atmos. Meas. Tech.* **2017**, *10*, 3575.
- (19) Holstius, D. M.; Pillarisetti, A.; Smith, K. R.; Seto, E. Field calibrations of a low-cost aerosol sensor at a regulatory monitoring site in California. *Atmos. Meas. Tech.* **2014**, *7*, 1121–1131.
- (20) Mukherjee, A.; Brown, S. G.; McCarthy, M. C.; Pavlovic, N. R.; Stanton, L. G.; Snyder, J. L.; D'Andrea, S.; Hafner, H. R. Measuring Spatial and Temporal PM2.5 Variations in Sacramento, California, Communities Using a Network of Low-Cost Sensors. *Sensors* 2019, 19, 4701.
- (21) Gao, M.; Cao, J.; Seto, E. A distributed network of low-cost continuous reading sensors to measure spatiotemporal variations of PM2.5 in Xi'an, China. *Environ. Pollut.* **2015**, *199*, 56–65.
- (22) Heimann, I.; Bright, V. B.; McLeod, M. W.; Mead, M. I.; Popoola, O. A. M.; Stewart, G. B.; Jones, R. L. Source attribution of air pollution by spatial scale separation using high spatial density networks of low cost air quality sensors. *Atmos. Environ.* **2015**, *113*, 10–19.
- (23) SCAQMD, SCAQMD AQSPEC. Field Evaluation Purple Air PM Sensor, 2016.
- (24) SCAQMD, SCAQMD AQSPEC. Field EvaluationPurple Air (PA-II) PM Sensor. http://www.aqmd.gov/docs/default-source/aqspec/field-evaluations/purple-air-pa-ii---field-evaluation.pdf?sfvrsn=2 (accessed on September 1, 2021).
- (25) SCAQMD, SCAQMD AQSPEC. Laboratory Evaluation PurpleAir PA-I PM Sensor, 2016.
- (26) He, H.; Stehr, J. W.; Hains, J. C.; Krask, D. J.; Doddridge, B. G.; Vinnikov, K. Y.; Canty, T. P.; Hosley, K. M.; Salawitch, R. J.; Worden, H. M.; Dickerson, R. R. Trends in emissions and concentrations of air pollutants in the lower troposphere in the Baltimore/Washington airshed from 1997 to 2011. *Atmos. Chem. Phys.* 2013, 13, 7859–7874.
- (27) Ogulei, D.; Hopke, P. K.; Zhou, L.; Patrick Pancras, J.; Nair, N.; Ondov, J. M. Source apportionment of Baltimore aerosol from combined size distribution and chemical composition data. *Atmos. Environ.* **2006**, *40*, 396–410.
- (28) Sarnat, J. A.; Koutrakis, P.; Suh, H. H. Assessing the relationship between personal particulate and gaseous exposures of senior citizens living in Baltimore, MD. *J. Air Waste Manage. Assoc.* **2000**, *50*, 1184–1198.
- (29) Williams, R.; Creason, J.; Zweidinger, R.; Watts, R.; Sheldon, L.; Shy, C. Indoor, outdoor, and personal exposure monitoring of particulate air pollution: the Baltimore elderly epidemiology-exposure pilot study. *Atmos. Environ.* **2000**, *34*, 4193–4204.
- (30) Yli-Pelkonen, V.; Scott, A. A.; Viippola, V.; Setälä, H. Trees in urban parks and forests reduce O3, but not NO2 concentrations in Baltimore, MD, USA. *Atmos. Environ.* **2017**, *167*, 73–80.
- (31) Environment, MDot. https://mde.maryland.gov/programs/Air/AirQualityMonitoring/Documents/MDNetworkPlanCY2022.pdf; Spring 2021: mde.maryland.gov, March 17, 2021.
- (32) Schwarz, G. Estimating the dimension of a model. *Ann. Stat.* **1978**, *6*, 461–464.

- (33) Zamora, M. L.; Rice, J.; Koehler, K. One year evaluation of three low-cost PM2.5 monitors. *Atmos. Environ.* **2020**, 235, 117615.
- (34) Soneja, S.; Chen, C.; Tielsch, J.; Katz, J.; Zeger, S.; Checkley, W.; Curriero, F.; Breysse, P. Humidity and gravimetric equivalency adjustments for nephelometer-based particulate matter measurements of emissions from solid biomass fuel use in cookstoves. *Int. J. Environ. Res. Public Health* **2014**, *11*, 6400–6416.
- (35) Sayahi, T.; Butterfield, A.; Kelly, K. E. Long-term field evaluation of the Plantower PMS low-cost particulate matter sensors. *Environ. Pollut.* **2019**, 245, 932–940.
- (36) Zuidema, C.; Sousan, S.; Stebounova, L. V.; Gray, A.; Liu, X.; Tatum, M.; Stroh, O.; Thomas, G.; Peters, T.; Koehler, K. Mapping Occupational Hazards with a Multi-sensor Network in a Heavy-Vehicle Manufacturing Facility. *Ann. Work Exposures Health* **2019**, *63*, 280–293.
- (37) EPA. 40 CFR Parts 53-General Requirements for an Equivalent Method Determination (Subchapter C); Environmental Protection Agency: Washington, DC, 2006.
- (38) EPA. Criteria Air Pollutants National Ambient Air Quality Standards (NAAQS) Table. https://www.epa.gov/criteria-air-pollutants/naaqs-table (accessed on September 1, 2021).
- (39) Duvall, R.; Clements, A.; Hagler, G.; Kamal, A.; Kilaru, V.; Goodman, L.; Frederick, S.; Barkjohn, K.; VonWald, I.; Greene, D. Performance Testing Protocols, Metrics, and Target Values for Fine Particulate Matter Air Sensors: Use in Ambient, Outdoor, Fixed Sites, Non-Regulatory Supplemental and Informational Monitoring Applications; US EPA Office of Research and Development, 2021.
- (40) Austin, E.; Novosselov, I.; Seto, E.; Yost, M. G. Laboratory Evaluation of the Shinyei PPD42NS Low-Cost Particulate Matter Sensor. *PLoS One* **2015**, *10*, No. e0137789.
- (41) Chakrabarti, B.; Fine, P. M.; Delfino, R.; Sioutas, C. Performance evaluation of the active-flow personal DataRAM PM2.5 mass monitor (Thermo Anderson pDR-1200) designed for continuous personal exposure measurements. *Atmos. Environ.* **2004**, 38, 3329–3340.
- (42) Feenstra, B.; Papapostolou, V.; Hasheminassab, S.; Zhang, H.; Boghossian, B. D.; Cocker, D.; Polidori, A. Performance evaluation of twelve low-cost PM2.5 sensors at an ambient air monitoring site. *Atmos. Environ.* **2019**, *216*, 116946.
- (43) Kelly, K. E.; Whitaker, J.; Petty, A.; Widmer, C.; Dybwad, A.; Sleeth, D.; Martin, R.; Butterfield, A. Ambient and laboratory evaluation of a low-cost particulate matter sensor. *Environ. Pollut.* **2017**, 221, 491–500.
- (44) Manikonda, A.; Zíková, N.; Hopke, P. K.; Ferro, A. R. Laboratory assessment of low-cost PM monitors. *J. Aerosol Sci.* **2016**, 102, 29–40.
- (45) Liu, X.; Jayaratne, R.; Thai, P.; Kuhn, T.; Zing, I.; Christensen, B.; Lamont, R.; Dunbabin, M.; Zhu, S.; Gao, J.; Wainwright, D.; Neale, D.; Kan, R.; Kirkwood, J.; Morawska, L. Low-cost sensors as an alternative for long-term air quality monitoring. *Environ. Res.* **2020**, 185, 109438.
- (46) Sousan, S.; Koehler, K.; Hallett, L.; Peters, T. M. Evaluation of consumer monitors to measure particulate matter. *J. Aerosol Sci.* **2017**, *107*, 123–133.
- (47) Sousan, S.; Koehler, K.; Hallett, L.; Peters, T. M. Evaluation of the Alphasense Optical Particle Counter (OPC-N2) and the Grimm Portable Aerosol Spectrometer (PAS-1.108). *Aerosol Sci. Technol.* **2016**, *50*, 1352–1365.
- (48) Chatzidiakou, L.; Krause, A.; Popoola, O. A. M.; Di Antonio, A.; Kellaway, M.; Han, Y.; Squires, F. A.; Wang, T.; Zhang, H.; Wang, Q.; Fan, Y.; Chen, S.; Hu, M.; Quint, J. K.; Barratt, B.; Kelly, F. J.; Zhu, T.; Jones, R. L. Characterising low-cost sensors in highly portable platforms to quantify personal exposure in diverse environments. *Atmos. Meas. Tech.* **2019**, *12*, 4643.
- (49) Giordano, M. R.; Malings, C.; Pandis, S. N.; Presto, A. A.; McNeill, V. F.; Westervelt, D. M.; Beekmann, M.; Subramanian, R. From low-cost sensors to high-quality data: A summary of challenges and best practices for effectively calibrating low-cost particulate matter mass sensors. *J. Aerosol Sci.* 2021, 158, 105833.

- (50) Romero, Y.; Velásquez, R. M. A.; Noel, J. Development of a multiple regression model to calibrate a low-cost sensor considering reference measurements and meteorological parameters. *Environ. Monit. Assess.* **2020**, *192*, 498.
- (51) Si, M.; Xiong, Y.; Du, S.; Du, K. Evaluation and calibration of a low-cost particle sensor in ambient conditions using machine-learning methods. *Atmos. Meas. Tech.* **2020**, *13*, 1693–1707.
- (52) Datta, A.; Saha, A.; Zamora, M. L.; Buehler, C.; Hao, L.; Xiong, F.; Gentner, D. R.; Koehler, K. Statistical field calibration of a low-cost PM2.5 monitoring network in Baltimore. *Atmos. Environ.* **2020**, *242*, 117761
- (53) Lee, H.; Kang, J.; Kim, S.; Im, Y.; Yoo, S.; Lee, D. Long-Term Evaluation and Calibration of Low-Cost Particulate Matter (PM) Sensor. Sensors 2020, 20, 3617.
- (54) Bi, J.; Wildani, A.; Chang, H. H.; Liu, Y. Incorporating Low-Cost Sensor Measurements into High-Resolution PM2.5 Modeling at a Large Spatial Scale. *Environ. Sci. Technol.* **2020**, *54*, 2152–2162.
- (55) Barkjohn, K. K.; Gantt, B.; Clements, A. L. Development and application of a United States-wide correction for PM2.5 data collected with the PurpleAir sensor. *Atmos. Meas. Tech.* **2021**, *14*, 4617–4637.
- (56) Tryner, J.; L'Orange, C.; Mehaffy, J.; Miller-Lionberg, D.; Hofstetter, J. C.; Wilson, A.; Volckens, J. Laboratory evaluation of low-cost PurpleAir PM monitors and in-field correction using colocated portable filter samplers. *Atmos. Environ.* **2020**, 220, 117067.
- (57) Wang, K.; Chen, F.-e.; Au, W.; Zhao, Z.; Xia, Z.-l. Evaluating the feasibility of a personal particle exposure monitor in outdoor and indoor microenvironments in Shanghai, China. *Int. J. Environ. Health Res.* **2019**, 29, 209–220.
- (58) Bulot, F. M.; Johnston, S. J.; Basford, P. J.; Easton, N. H.; Apetroaie-Cristea, M.; Foster, G. L.; Morris, A. K.; Cox, S. J.; Loxham, M. Long-term field comparison of multiple low-cost particulate matter sensors in an outdoor urban environment. *Sci. Rep.* **2019**, *9*, 7497.
- (59) Alphasense Ltd. CO-A4 Carbon Monoxide Sensor 4-Electrode. http://www.alphasense.com/WEB1213/wp-content/uploads/2015/01/COA4.pdf (accessed on September 1, 2021).
- (60) Williams, R.; Kilaru, V.; Snyder, E.; Kaufman, A.; Dye, T.; Rutter, A.; Russel, A.; Hafner, H. *Air Sensor Guidebook*; US Environmental Protection Agency: Washington, DC; EPA/600/R-14/159 (NTIS PB2015-100610), 2014.
- (61) Zamora, M. L.; Zuidema, C.; Koehler, K. Sensor. *Patty's Industrial Hygiene*; Wiley, 2020; pp 1–16.
- (62) Castell, N.; Dauge, F. R.; Schneider, P.; Vogt, M.; Lerner, U.; Fishbain, B.; Broday, D.; Bartonova, A. Can commercial low-cost sensor platforms contribute to air quality monitoring and exposure estimates? *Environ. Int.* **2017**, *99*, 293–302.
- (63) Alhasa, K.; Mohd Nadzir, M.; Olalekan, P.; Latif, M.; Yusup, Y.; Iqbal Faruque, M.; Ahamad, F.; Abd Hamid, H.; Aiyub, K.; Md Ali, S.; Khan, M.; Abu Samah, A.; Yusuff, I.; Othman, M.; Tengku Hassim, T.; Ezani, N. Calibration model of a low-cost air quality sensor using an adaptive neuro-fuzzy inference system. *Sensors* 2018, 18, 4380.
- (64) Addabbo, T.; Fort, A.; Mugnaini, M.; Parri, L.; Parrino, S.; Pozzebon, A.; Vignoli, V. An IoT Framework for the Pervasive Monitoring of Chemical Emissions in Industrial Plants. 2018 Workshop on Metrology for Industry 4.0 and IoT, 16–18 April 2018; IEEE, 2018; pp 269–273.
- (65) Samad, A.; Obando Nuñez, D. R.; Solis Castillo, G. C.; Laquai, B.; Vogt, U. Effect of Relative Humidity and Air Temperature on the Results Obtained from Low-Cost Gas Sensors for Ambient Air Quality Measurements. Sensors 2020, 20, 5175.
- (66) Jiao, W.; Hagler, G.; Williams, R.; Sharpe, R.; Brown, R.; Garver, D.; Judge, R.; Caudill, M.; Rickard, J.; Davis, M.; Weinstock, L.; Zimmer-Dauphinee, S.; Buckley, K. Community Air Sensor Network (CAIRSENSE) project: evaluation of low-cost sensor performance in a suburban environment in the southeastern United States. *Atmos. Meas. Tech.* **2016**, *9*, 5281–5292.
- (67) Zuidema, C.; Schumacher, C. S.; Austin, E.; Carvlin, G.; Larson, T. V.; Spalt, E. W.; Zusman, M.; Gassett, A. J.; Seto, E.; Kaufman, J. D.; Sheppard, L. Deployment, Calibration, and Cross-

Validation of Low-Cost Electrochemical Sensors for Carbon Monoxide, Nitrogen Oxides, and Ozone for an Epidemiological Study. Sensors 2021, 21, 4214.

- (68) Mauderly, J. L.; Burnett, R. T.; Castillejos, M.; Özkaynak, H.; Samet, J. M.; Stieb, D. M.; Vedal, S.; Wyzga, R. E. Is the air pollution health research community prepared to support a multipollutant air quality management framework? *Inhal. Toxicol.* **2010**, 22, 1–19.
- (69) van Zoest, V.; Osei, F. B.; Stein, A.; Hoek, G. Calibration of low-cost NO2 sensors in an urban air quality network. *Atmos. Environ.* **2019**, *210*, 66–75.
- (70) Kim, J.; Shusterman, A. A.; Lieschke, K. J.; Newman, C.; Cohen, R. C. The BErkeley Atmospheric CO2 Observation Network: field calibration and evaluation of low-cost air quality sensors. *Atmos. Meas. Tech.* **2018**, *11*, 1937–1946.
- (71) Ripoll, A.; Viana, M.; Padrosa, M.; Querol, X.; Minutolo, A.; Hou, K. M.; Barcelo-Ordinas, J. M.; García-Vidal, J. Testing the performance of sensors for ozone pollution monitoring in a citizen science approach. *Sci. Total Environ.* **2019**, *651*, 1166–1179.
- (72) Morawska, L.; Thai, P. K.; Liu, X.; Asumadu-Sakyi, A.; Ayoko, G.; Bartonova, A.; Bedini, A.; Chai, F.; Christensen, B.; Dunbabin, M.; Gao, J.; Hagler, G. S. W.; Jayaratne, R.; Kumar, P.; Lau, A. K. H.; Louie, P. K. K.; Mazaheri, M.; Ning, Z.; Motta, N.; Mullins, B.; Rahman, M. M.; Ristovski, Z.; Shafiei, M.; Tjondronegoro, D.; Westerdahl, D.; Williams, R. Applications of low-cost sensing technologies for air quality monitoring and exposure assessment: How far have they gone? *Environ. Int.* 2018, 116, 286–299.
- (73) Spinelle, L.; Gerboles, M.; Aleixandre, M. Performance Evaluation of Amperometric Sensors for the Monitoring of O 3 and NO 2 in Ambient Air at ppb Level. *Procedia Eng.* **2015**, *120*, 480–483.
- (74) Baron, R.; Saffell, J. Amperometric gas sensors as a low cost emerging technology platform for air quality monitoring applications: A review. ACS Sens. 2017, 2, 1553–1566.
- (75) Orellano, P.; Reynoso, J.; Quaranta, N.; Bardach, A.; Ciapponi, A. Short-term exposure to particulate matter (PM10 and PM2.5), nitrogen dioxide (NO2), and ozone (O3) and all-cause and cause-specific mortality: Systematic review and meta-analysis. *Environ. Int.* **2020**, *142*, 105876.

☐ Recommended by ACS

New Insights for Tracking Global and Local Trends in Exposure to Air Pollutants

Martin J. Wolf, John W. Emerson, et al.

MARCH 07, 2022

ENVIRONMENTAL SCIENCE & TECHNOLOGY

READ 🗹

Impacts of Personal Mobility and Diurnal Concentration Variability on Exposure Misclassification to Ambient Pollutants

Rakefet Shafran-Nathan, David M. Broday, et al.

MARCH 02, 2018

ENVIRONMENTAL SCIENCE & TECHNOLOGY

READ

A Network of Field-Calibrated Low-Cost Sensor Measurements of PM2.5 in Lomé, Togo, Over One to Two Years

Garima Raheja, Daniel M. Westervelt, et al.

MARCH 10, 2022

ACS EARTH AND SPACE CHEMISTRY

READ 🗹

Near-Road Air Pollutant Measurements: Accounting for Inter-Site Variability Using Emission Factors

Jonathan M. Wang, Greg J. Evans, et al.

JULY 19, 2018

ENVIRONMENTAL SCIENCE & TECHNOLOGY

READ 🗹

Get More Suggestions >